

Injection of carbon from the shelf to offshore beneath the euphotic zone in the California Current

John A. Barth, Timothy J. Cowles, P. Michael Kosro, R. Kipp Shearman, Adriana Huyer, and Robert L. Smith

College of Oceanic and Atmospheric Sciences, Oregon State University, Corvallis, Oregon, USA

Received 4 May 2001; revised 7 August 2001; accepted 22 August 2001; published 25 June 2002.

[1] High concentrations of chlorophyll are found in the California Current System over 300 km offshore, far from the productive coastal upwelling region, and between 150 and 250 m, well below the depth to which photosynthetically active solar radiation penetrates. This exceptionally deep chlorophyll feature is formed near the coast and transported offshore in the meandering California Current jet. Chlorophyll is forced downward along sloping density surfaces through conservation of potential vorticity along the meandering jet path. Thus mesoscale physical dynamics serve to inject large amounts of carbon, e.g., 2400 t as reported here, per event from regions of active coastal upwelling into the adjacent deep ocean, a process that must be considered when computing oceanic carbon budgets.

INDEX TERMS: 4520 Oceanography: Physical: Eddies and mesoscale processes; 4528 Oceanography: Physical: Fronts and jets; 4806 Oceanography: Biological and Chemical: Carbon cycling; *KEYWORDS:* upwelling, meanders, mesoscale, jet(s), chlorophyll, carbon

1. Introduction

[2] Eastern boundary current regions of the world's oceans are highly productive because of their proximity to coastal upwelling zones over the shallow shelf adjacent to continental boundaries. Satellite sea surface temperature (SST) imagery and in situ measurements have shown the existence of cold filaments extending offshore from the coastal upwelling zone to the adjacent deep ocean [Bernstein *et al.*, 1977]. These features often have high phytoplankton biomass and nutrients near the surface [Traganza *et al.*, 1981] and have been the focus of several recent studies [Brink and Cowles, 1991]. Cold, filamentous features stretching seaward from coastal upwelling zones are a universal phenomenon of eastern boundary current regions, having been documented in the southeast Atlantic [Shillington *et al.*, 1990], the northeast Atlantic [Haynes *et al.*, 1993], and the southeast Pacific [Strub *et al.*, 1998]. In this paper the characteristics, origin, and implications for off-shelf carbon flux of an exceptionally deep chlorophyll feature in the California Current System (CCS), the eastern boundary current of the subtropical North Pacific [Wooster and Reid, 1963], are reported.

2. Data and Analysis Methods

[3] During June and July 1993, measurements of temperature, salinity, and pressure were made from the towed vehicle SeaSoar [Pollard, 1986] undulating between 0 and 300 m. Details of the data processing are reported by Huyer *et al.* [1998].

[4] Chlorophyll *a* (Chl *a*) fluorescence was measured from the same platform using a single-wavelength (660 nm) fluorometer (6–19 June) and a new multiwavelength fluorescence instrument (21 June to 2 July) [Cowles *et al.*, 1994]. Fluorescence was converted to concentration (mg m^{-3}) through calibration with discrete water samples filtered and measured for chlorophyll [Kosro *et al.*, 1995]. Two fluorescence emission ratios were obtained with the multiwavelength fluorometer that used 430, 487, and 520 nm excitation (20 nm bandpass) and measured photosynthetic pigment emission at 685 nm (the peak emission maximum for Chl *a*). A blue:violet ratio was obtained by using quantum-corrected fluorescence emission at 685 nm based on 487 nm (blue) excitation divided by the quantum-corrected emission at 685 nm based on 430 nm (violet) excitation. Similarly, a green:violet ratio was obtained by using 520 (green) and 430 nm (violet) excitations. Changes in these ratios as a function of depth may reflect taxonomic differences between phytoplankton assemblages or may reflect photoadaptive responses to alterations in the local irradiance field [Neori *et al.*, 1984].

[5] The SeaSoar vehicle completed one profiling cycle every 10 min, yielding an alongtrack resolution of 2.5 km or less. Measurements were averaged vertically to 2 dbar bins. The spatially averaged temperature, salinity, and pressure data are used to compute geopotential anomaly (dynamic height in meters multiplied by the acceleration of gravity) in $\text{J kg}^{-1} (\text{m}^2 \text{s}^{-2})$ relative to a chosen reference level.

3. Results

[6] From 7 to 28 June a 400 by 400 km region of the CCS offshore of the continental margin (500 m isobath) was surveyed from north to south [Huyer *et al.*, 1998] (Figure 1). During this period, winds were upwelling favorable, having

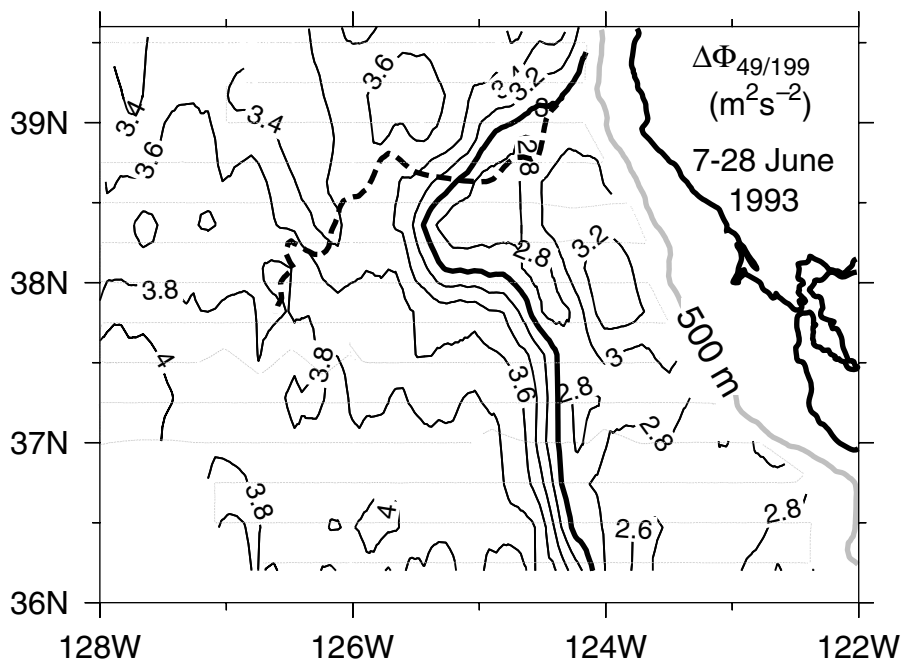


Figure 1. Geopotential anomaly at 49 m relative to 199 m, $\Delta\Phi_{49/199}$ ($\text{m}^2 \text{s}^{-2}$), during 7–28 June 1993. Data locations, sampled from north to south, are indicated by small dots. The dashed curve denotes the equatorward jet location on 29 June 1993 derived from the SST front evident in Figure 3c.

become so around 5 June (Figure 2). Satellite SST imagery from late May shows relatively little cold water near the coast, indicating a lack of upwelling except in a series of cyclonic (counterclockwise) eddies, one of which formed near Point Arena, California (39°N) (Figure 3a). SST images from June reveal a band of cold water from active upwelling near the coast (Figures 3b and 3c). Geostrophic flow is along contours of geopotential anomaly, and an equatorward meandering jet is apparent in a map of geopotential anomaly at 49 m relative to 199 m ($\Delta\Phi_{49/199}$ $\text{m}^2 \text{s}^{-2}$) (Figure 1).

[7] Chl *a* concentrations from SeaSoar crossings of the equatorward jet axis ($\Delta\Phi_{49/199} = 3.0 \text{ m}^2 \text{s}^{-2}$) show enhanced values in water with density anomaly of 25.0 kg m^{-3} and

lighter (Figure 4). This density range is shallower than about 75 m and within the euphotic zone. Nowhere along the jet, or along 38.25° or 38.5°N zonal lines passing through the cyclonic feature ($\Delta\Phi_{49/199} < 2.8 \text{ m}^2 \text{s}^{-2}$) on the inshore side of the jet near 125°W , do high chlorophyll concentrations appear deeper than 75 m.

[8] The thermohaline and velocity structure of the CCS is time-dependent [Huyer *et al.*, 1998] as evident by changes in the location of the meandering jet during June. The position of an isotherm at the offshore edge of the region of cold, upwelled water bounded by the meandering equatorward jet on 29 June 1993 (Figure 3c) indicates that the jet near 38.5°N had moved offshore since 11–16 June when it was sampled by ship (Figure 1). The farthest offshore extent

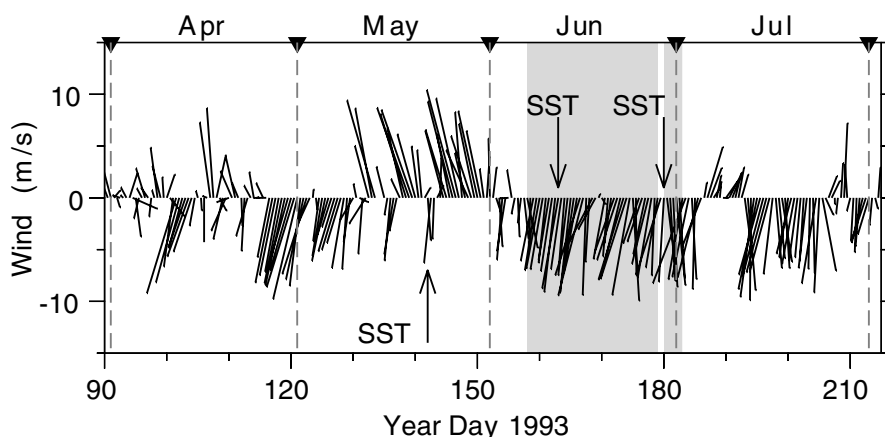


Figure 2. Vector winds during 1993 measured at Point Arena, California (38.95°N), rotated so that up is toward 353°T . Ship measurement periods are shown as shaded bars, and the times of the SST images in Figure 3 are indicated by arrows.

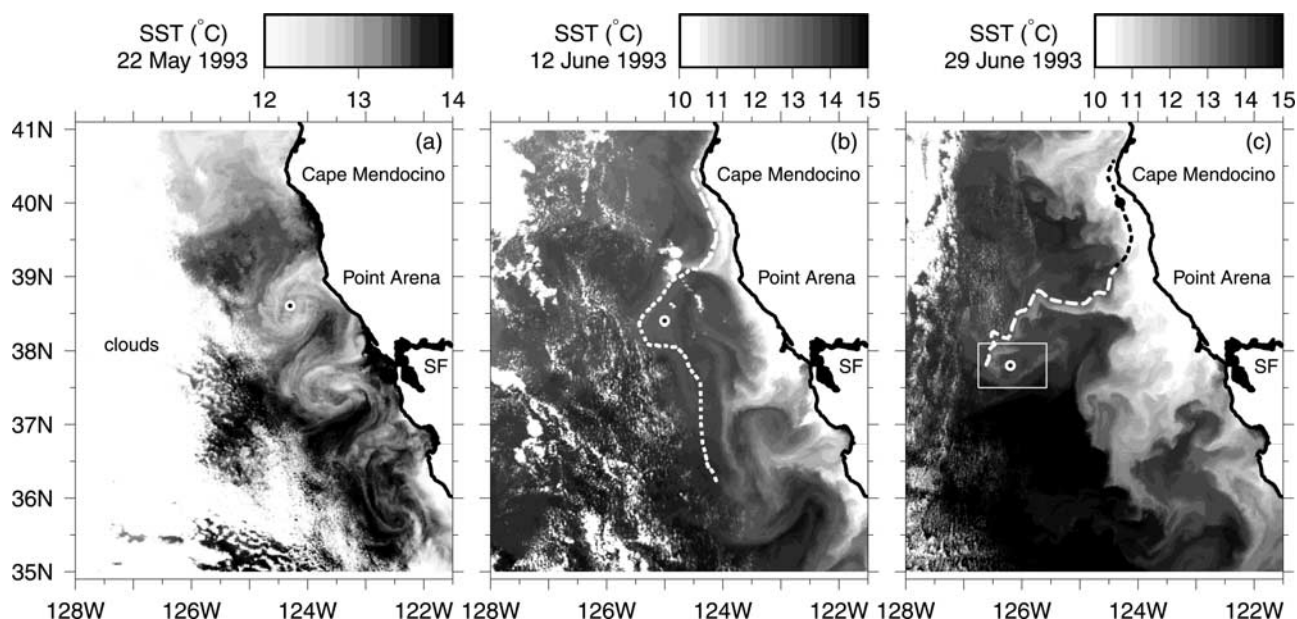


Figure 3. (a) Satellite SST image from 2300 UTC, 22 May 1993. (b) Satellite SST image from 0000 UTC, 12 June 1993. The white dashed curve is the 12°C contour, and the white dotted curve is the location of the center of the meandering equatorward jet as sampled by ship from 7 to 28 June 1993 (see Figure 1). (c) SST image from 2300 UTC, 29 June 1993. The white dashed curve is the 13.45°C contour on 29 June, and the black dashed curve is the 12°C contour from the 12 June SST image. Vertical sections were collected in the box centered near 37.75°N, 126.25°W during 29 June to 2 July, and the black dot near Cape Mendocino is 400 km upstream of the box. In each panel the center of the cyclonic eddy is marked with a black and white bullet.

of the jet is marked by a sharp cyclonic turn back to the east near 126.5°W. This region was surveyed in detail using SeaSoar during 29 June to 2 July 1993 [Shearman *et al.*, 1999].

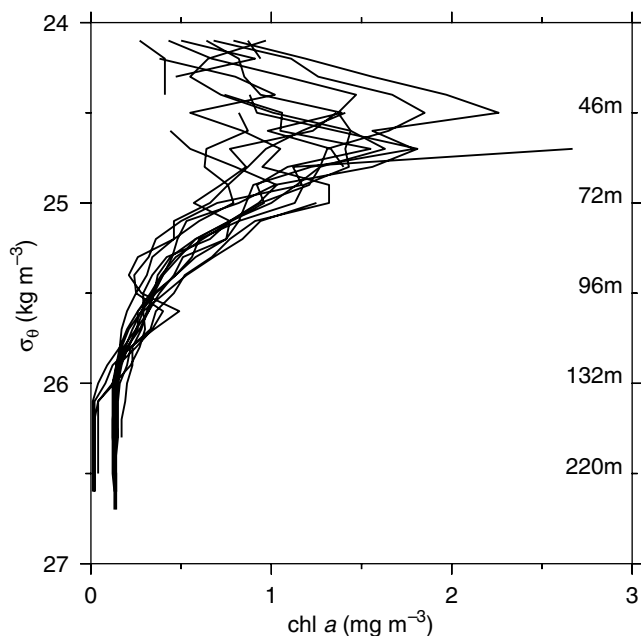


Figure 4. Chl *a* (mg m^{-3}) derived from fluorescence as a function of density anomaly (kg m^{-3}) from the center ($\Delta\Phi_{49/199} = 3.0 \text{ m}^2 \text{ s}^{-2}$) of the meandering equatorward jet for each east-west line in Figure 1. Indicated depths are for a density profile from the jet center at 38.5°N.

[9] A vertical section of Chl *a* concentration across the jet in the cyclonic meander (Figure 5a) shows high values in the surface layer, consistent with those found during the 7–28 June survey, but also a large maximum (values exceeding 2 mg m^{-3}) between 150 and 250 m. The deep maximum is separated from the surface maximum, indicating that local sinking of phytoplankton across density surfaces is an unlikely source. Furthermore, there was a significant difference in the fluorescence emission ratios between the phytoplankton populations found at 45 m and those found at 200 m, suggesting that these populations had different light absorption spectra, reflecting either different light history regimes or different species assemblages. The deep feature is 40 km wide and is located within the southward flowing jet as indicated by the geopotential anomaly gradient and southward (<0) geostrophic velocity (Figure 5b). The deep, high-chlorophyll feature is found in the density anomaly range $26.0\text{--}26.7 \text{ kg m}^{-3}$, again distinct from the surface chlorophyll maximum occupying waters with density anomaly $<25.6 \text{ kg m}^{-3}$ (Figure 6).

[10] A second, significantly smaller, isolated subsurface chlorophyll maximum (peak values of 1.0 mg m^{-3}) is found around 100–150 m, between 125.73° and 126.14°W (Figure 5a). This feature occupies the lighter end of the $26.0\text{--}26.7 \text{ kg m}^{-3}$ density anomaly range and is associated with the counterclockwise eddy within the cyclonic meander of the jet (Figure 5b). For a density interval encompassing the deep chlorophyll maxima ($26.2\text{--}26.5 \text{ kg m}^{-3}$), warm, salty anomalies of similar magnitude are found in both the southward jet and the cyclonic eddy. The fluorescence emission ratios of the phytoplankton found at the 26.4 density anomaly were not significantly different within the

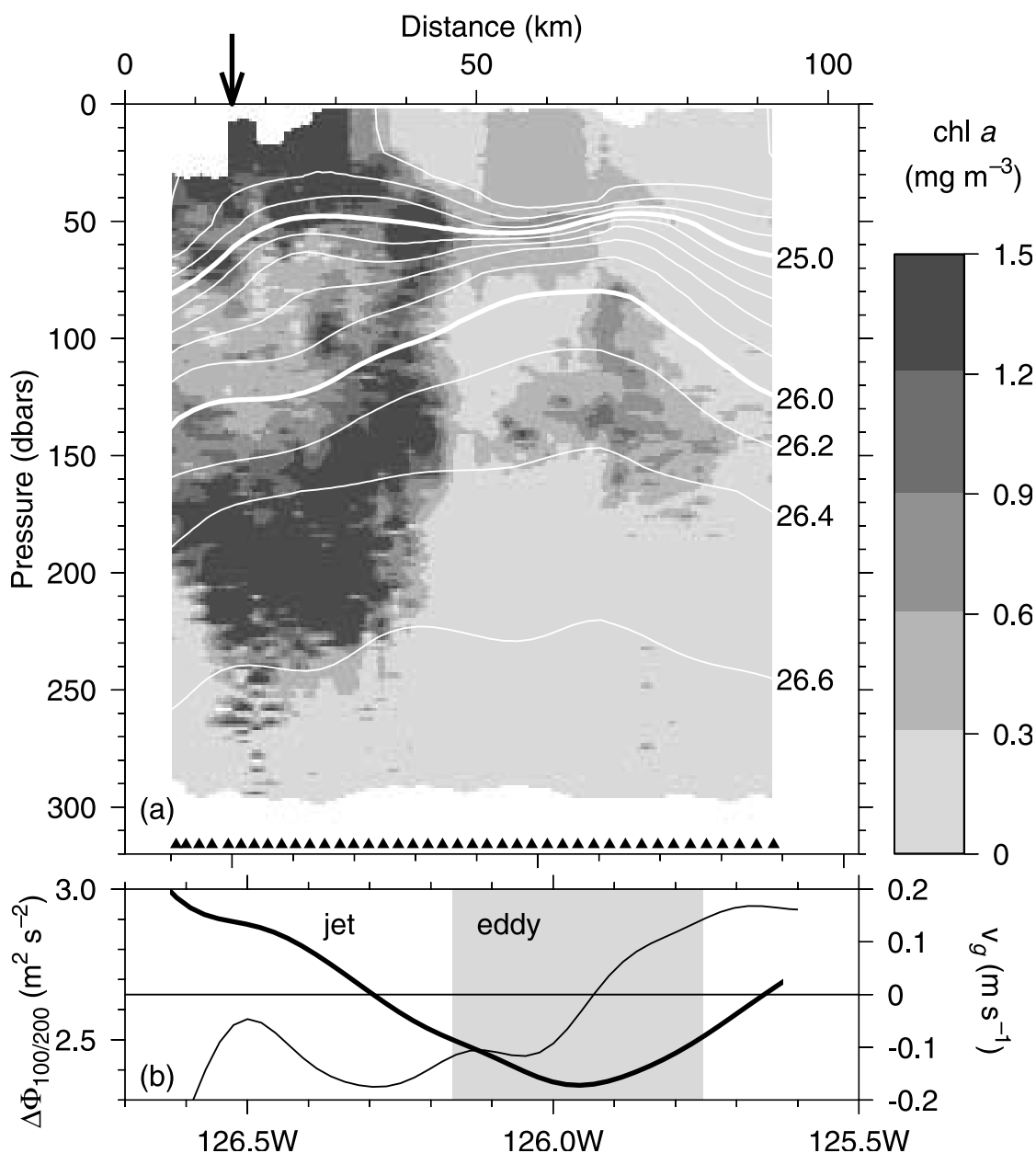


Figure 5. (a) Vertical section of Chl *a* (mg m^{-3}) derived from fluorescence (color) along 37.87°N on 30 June 1993 overlaid with contours of density anomaly (kg m^{-3}). The locations of each SeaSoar up-down cycle are indicated by triangles along the bottom. (b) Geopotential anomaly at 100 m, $\Delta\Phi_{100/200}$ ($\text{m}^2 \text{s}^{-2}$) (thick curve), and 100 m north-south geostrophic velocity, v_g (m s^{-1}), both referenced to acoustic Doppler current profiler velocity at 200 m, along 37.87°N . See color version of this figure at back of this issue.

jet and the eddy. Thus distinguishing these water masses by their thermohaline or fluorescence properties is difficult.

[11] The alongjet horizontal extent of the deep chlorophyll maximum is evident in maps of Chl *a* concentration within the two distinct density anomaly ranges $24.5\text{--}25.6$ (average depth of 66 m) and $26.0\text{--}26.7$ (average depth of 204 m) kg m^{-3} (Figure 7). The deep maximum is roughly circular and extends about 40–50 km in the north-south (alongjet) direction. Upstream of the deep maximum (to the NE), chlorophyll concentrations on the deep density anomaly surface are only slightly elevated, while downstream there is a sharp boundary to the feature. The deep maximum

is in the southward flowing jet as evident from contours of geopotential anomaly. The weaker subsurface maximum associated with the eddy ($\Delta\Phi_{100/200} \leq 2.5 \text{ m}^2 \text{ s}^{-2}$) is just visible (Figure 7b).

[12] The surface chlorophyll maximum is found within the jet, and in the eddy, although to a lesser extent, from the farthest NE measurements to about 37.5°N (Figure 7a). The surface maximum is not found downstream of about 126.2°W after the jet has turned to the E-NE. The two maxima are not aligned vertically, although the regions of increased chlorophyll concentration have substantial overlap. The westward displacement of the deep maximum

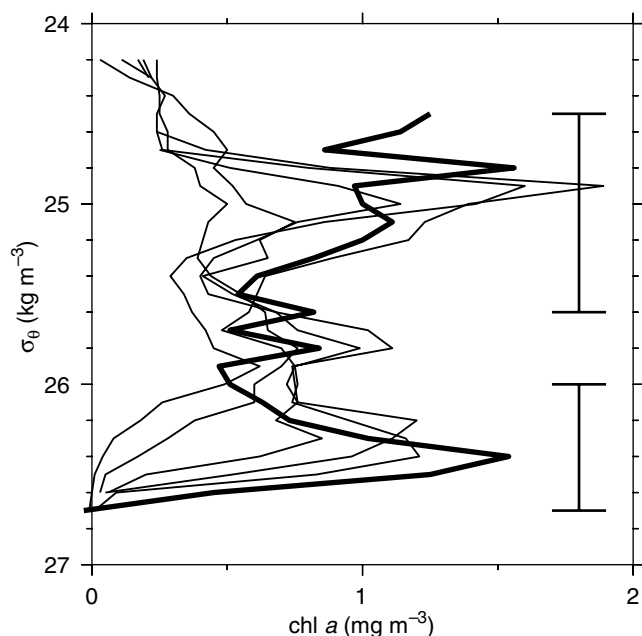


Figure 6. Chl *a* (mg m^{-3}) as a function of density anomaly (kg m^{-3}) at the meandering jet core ($\Delta\Phi_{100/200} = 2.9 \text{ m}^2 \text{ s}^{-2}$) from sections between 37.6° and 38.1°N (see Figure 7 for locations). The thick curve is from 37.87°N , indicated by an arrow in Figure 5, and vertical bars indicate σ_θ averaging intervals used for Figure 7.

relative to the surface maximum is consistent with movement down the sloping isopycnals.

4. Discussion

[13] The above description motivates the consideration of the origin of this exceptionally deep (150–250 m) chlorophyll maximum. The feature lies beneath the surface euphotic zone, so production at depth is ruled out. The deep chlorophyll maximum is isolated from the surface maximum, as noted earlier, so local sinking from above is unlikely. The density anomaly surface 26.4 kg m^{-3} on which the deep chlorophyll maximum is centered does not approach closer than within 140 m of the sea surface within the large-scale survey region [Huyer *et al.*, 1998]. Thus production in the euphotic zone offshore of the continental slope and transport to depth within the survey region is not possible. The only place where this isopycnal approaches to within 50 m of the surface is near the coast over the continental shelf during active upwelling [Huyer, 1984]. The ship survey did not approach closer to shore than the 1000 m isobath and only reached north to 39.5°N . To trace the center of the meandering jet farther upstream in order to find the origin of the deep chlorophyll maximum feature, an isotherm (12°C) from an SST image on 0000 12 June 1993 is used (Figure 3b). The 12°C isotherm on 12 June in the region 39.0° – 39.5°N matches well with the center of the meandering jet ($\Delta\Phi_{49/199} = 3.0 \text{ m}^2 \text{ s}^{-2}$) as determined by ship sampling on 7–11 June (Figure 3b). To determine the location of the jet core during the sampling of the deep chlorophyll feature (29 June to 2 July), the 13.45°C isotherm south of 39°N from a SST image on 29 June is

connected to the 12 June 12°C isotherm (Figure 3c). Thus a plausible complete path followed by the deep chlorophyll feature from over the continental shelf to its observed location near 38°N , 126.5°W is shown as a dashed curve in Figure 3c. Although the equatorward jet is vertically sheared, using an average jet speed of 0.2 m s^{-1} and the distance along the meandering jet from the point where the deep chlorophyll maximum was observed back to the coast (Figure 3c), a distance of 430 km was traversed in 25 days. This places a likely origin for the deep feature near the surface off Cape Mendocino (40.5°N) around 5 June, consistent with the beginning of the strong upwelling favorable wind period (Figure 2). The northern and coastal origin of the deep chlorophyll maximum and its subsequent advection in the meandering equatorward jet placed it upstream of the ship's location throughout the 7–28 June large-scale survey, hence the lack of deep chlorophyll observations during that period (Figure 4).

[14] Extended light limitation of photosynthesis does not prohibit the survival, nor the ability to fluoresce, of phytoplankton assemblages found at depth for periods of at least 2 months [Murphy and Cowles, 1997]. Therefore a coastal origin for the deep chlorophyll maximum observed here is possible. However, because Chl *a* fluorescence and Chl *a* fluorescence per cell level out after about 2 weeks in the dark, it is not possible to use fluorescence to estimate the time beyond 2 weeks since a chlorophyll-rich water parcel left the euphotic zone [Murphy and Cowles, 1997].

[15] The descent of the high-chlorophyll patch from near the surface ($\sim 50 \text{ m}$) to a center depth of 200 m implies a downwelling velocity of 6 m d^{-1} . This value is comparable to net downwelling rates of 7 – 15 m day^{-1} as diagnosed dynamically from density and velocity measurements of the cyclonic (positive relative vorticity) meander and adjacent cyclonic eddy [Shearman *et al.*, 1999]. Downwelling results from the conservation of potential vorticity as water columns slide down the sloping isopycnals (the slope exists because the density field is in geostrophic balance with the eastern boundary current jet) in response to an increase in their relative vorticity. Of course, upwelling occurs where the meandering jet enters anticyclonic curvature, but in a fully developed filament, modeling results suggest that downwelling predominates along a meandering jet path from its origin near the coast through a sharp cyclonic turn at its most offshore location [Haidvogel *et al.*, 1991]. Model predictions for downwelling velocity at 100 m are 5 – 10 m d^{-1} , again consistent with results reported here.

[16] Previous studies have documented the occurrence of downwelling in association with offshore jets in the CCS. Downwelling of 2 – 4 and 6 – 10 m d^{-1} along the 26.2 and 25.8 kg m^{-3} isopycnal surfaces, respectively, was inferred from observations of high chlorophyll, accompanied by high light attenuation, at depth [Washburn *et al.*, 1991]. In that study the deepest significant high-chlorophyll measurements ($>1.5 \text{ mg m}^{-3}$) were at 140 m, comparable to the shallowest extent of the deep chlorophyll maximum observed here. Higher values of vertical velocity have been estimated on the basis of chemical tracers (25 m d^{-1}) [Kadko *et al.*, 1991] and from the analysis of the response of mixed layer drifter clusters to changes in relative vorticity along a meandering jet path (20 m d^{-1}) [Swenson *et al.*, 1992]. These higher values are both associated with more

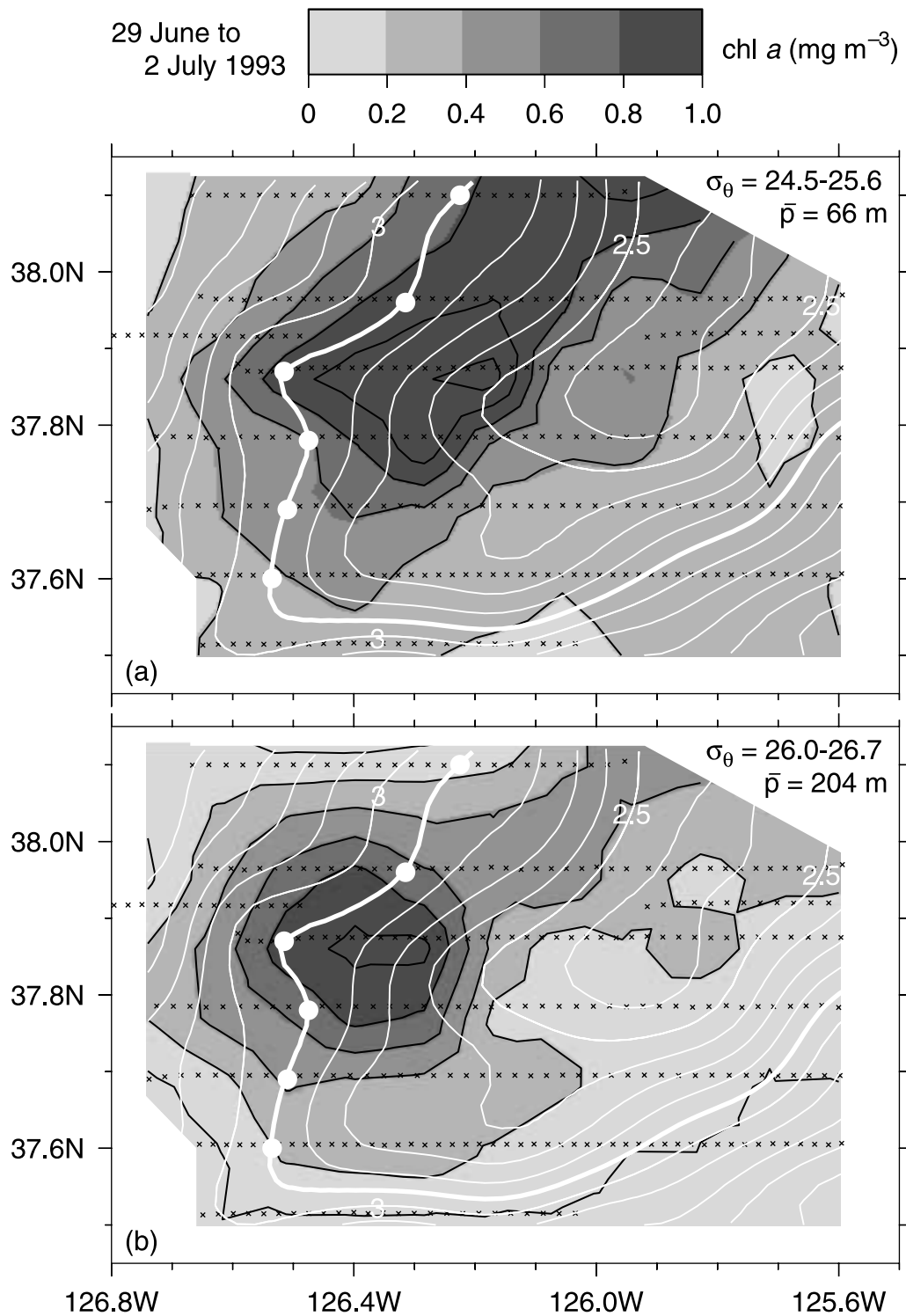


Figure 7. Chl *a* concentration (mg m^{-3}) derived from fluorescence (color and black contours) averaged between density anomaly surfaces (a) 24.5–25.6 and (b) 26.0–26.7 kg m^{-3} during 29 June to 2 July 1993 overlaid with contours of geopotential anomaly ($\text{m}^2 \text{s}^{-2}$) at 100 m referenced to acoustic Doppler current profiler velocity at 200 m (white contours). The thick geopotential anomaly contour ($2.9 \text{ m}^2 \text{s}^{-2}$) indicates the core of the meandering equatorward jet, and solid circles along this contour indicate locations of Chl *a* profiles shown in Figure 6. See color version of this figure at back of this issue.

localized regions than the net downwelling inferred along the 430 km path considered here and are consistent with diagnosed large vertical velocities (up to 40 m d^{-1}) on short spatial scales (20–30 km) [Shearman *et al.*, 1999].

[17] The role of sinking in the vertical displacement of phytoplankton from near the surface to depth must be considered. Reported values for sinking rates of oceanic phytoplankton are 1 m d^{-1} or less [Bienfang *et al.*, 1982;

Smayda, 1970]. Over a 25 day period this 25 m downward displacement is insufficient to account for the observation of high chlorophyll between 150 and 250 m. Allowing for sinking at 1 m d^{-1} would lower the estimate of vertical velocity to 5 m d^{-1} . As noted previously, the lack of phytoplankton between the deep and surface maxima (Figures 5 and 6) argues against sinking playing a major role.

[18] In a coastal upwelling zone the cross-jet horizontal scale for elevated chlorophyll, and hence carbon fixation through photosynthesis, is potentially as large as the region where nutrient-rich subsurface water rises into the euphotic zone. Off the west coast at 38.5°N , upwelling occurs within about 20 km of the coast [Huyer, 1984], while previous studies in other productive west coast upwelling zones (e.g., Oregon) show the region of elevated chlorophyll extending up to 40 km offshore [Small and Menzies, 1981]. This cross-jet scale is consistent with the observed width ($\sim 40 \text{ km}$) of the deep chlorophyll maximum (Figures 5 and 7). The along jet scale of the deep feature is more difficult to rationalize but is likely due to alongshore variations in the strength of upwelling (Figure 3), for example, from alongshore variations in the wind or irregularities in the coastline or bottom topography [Kelly, 1985; Barth et al., 2000; Samelson et al., 2002] or separately by or in consort with time variability in the wind forcing (Figure 2) or in the biological response to increased nutrient availability [MacIsaac et al., 1985].

[19] The warm, salty anomalies along density surfaces for the deep chlorophyll maximum in the jet and for the elevated chlorophyll around 125 m in the eddy are consistent with a coastal upwelling origin for both. The origin and pathway from the coast of the deep chlorophyll maximum in the jet has been described in detail. By examining SST imagery (e.g., Figure 3) the cyclonic eddy formed around 25 April 1993 near Point Arena (39°N) and translated W-SW at about 0.06 m s^{-1} . Thus 65 days elapsed between the eddy's formation near the coast and the detailed measurements presented here, considerably longer than the 25 days estimated for offshore movement of the deep chlorophyll maximum in the jet. The 65 day translation period would allow phytoplankton to sink 65 m, enough to account for a large percentage of the vertical displacement of this feature from the surface euphotic zone. Last, lower values of chlorophyll in the subsurface maximum in the eddy compared with those found deep in the jet are consistent with a longer period for zooplankton to graze down the phytoplankton biomass. In summary, phytoplankton sinking likely produced the deep chlorophyll feature in the cyclonic eddy, whereas the deep chlorophyll feature in the jet resulted from downwelling due to vorticity dynamics.

[20] The offshore flux of high-chlorophyll surface water from near the coast to depth as demonstrated here is likely an important mechanism for removing carbon from continental shelf ecosystems [Walsh et al., 1981]. Since up to 20–40% of the oceans primary productivity occurs over the continental shelves [Longhurst et al., 1995; Knauer, 1993], this export is important when considering oceanic carbon budgets [Liu et al., 2000]. An integration of the amount of chlorophyll present in the deep subsurface feature in the jet reported here yields $4.7 \times 10^4 \text{ kg Chl } a$, which, assuming a carbon:chlorophyll ratio of 50 [Landry and Lorenzen,

1989], equals $2.4 \times 10^6 \text{ kg}$ of carbon. In a coastal upwelling zone the amount of carbon integrated across the productive region within the euphotic zone and for 40 km alongshore is $1.3 \times 10^7 \text{ kg}$ [Small and Menzies, 1981]. The observed deep chlorophyll maximum thus represents a substantial fraction ($\sim 20\%$) of the carbon produced on the shelf. Given the certainty of phytoplankton biomass reduction by zooplankton grazing, this represents a lower bound for the offshore flux in this deep feature.

[21] The isolated, deep chlorophyll feature reported here is a good example of an episodic event which, given the likely scenario that the observed phytoplankton biomass will sink to the seafloor as particulate organic carbon, was hypothesized by Jahnke et al. [1990] to account for the underestimate of sediment trap-based estimates of downward organic carbon flux within 300 km of the coast off central California. The deep chlorophyll feature is limited in spatial extent and occurs episodically, hence the difficulty in observing particle fluxes from such events using sediment traps. Jahnke et al. [1990] estimate a benthic carbon mineralization rate of $0.8 \text{ mol C m}^{-2} \text{ yr}^{-1}$ within 300 km of the coast off central California. If the estimate of carbon contained in the deep chlorophyll feature ($2.4 \times 10^6 \text{ kg}$) is divided by the surface area of the roughly circular feature with a radius of 20 km, a concentration of $0.16 \text{ mol C m}^{-2}$ is obtained. Therefore the entire benthic mineralization rate could be supplied by a few of these events (~ 5) per year. Since the deep chlorophyll feature is well below the depth to which satellite ocean color sensors penetrate, they too will miss sampling these features.

[22] One final consideration is how common an occurrence this exceptionally deep chlorophyll maximum is in the CCS. Previous studies [Washburn et al., 1991] have described high-chlorophyll subsurface features in the CCS, reinforcing results presented here. As noted above, no deep features were found during the large-scale survey from 7 to 28 June, although small horizontal features may have been missed by the 28 km between-track spacing. Evidently, the switch from downwelling to upwelling favorable winds around 5 June and the subsequent biological response led to the formation of the high-chlorophyll feature documented here. Events of this nature happen several times per season (Figure 2), so it is hypothesized that offshore flux and injection to depth of high-chlorophyll shelf water by mesoscale physical dynamics occurs episodically throughout the upwelling season.

5. Summary and Conclusions

[23] High spatial resolution hydrographic and bio-optical measurements are used to document the existence of a deep, high-chlorophyll feature offshore in the California Current System. Chlorophyll concentrations in excess of 1.5 mg m^{-3} were found between 150 and 250 m, well below the depth to which light penetrates. The exceptionally deep high-chlorophyll feature was found over 300 km offshore of the coastal upwelling zone off central California. By examining the three-dimensional time-dependent flow field and the hydrographic and biological properties of the deep chlorophyll feature it is shown that the feature was formed near the coast and transported offshore in the meandering California Current jet. Chlorophyll is forced downward

along sloping density surfaces through the conservation of potential vorticity along the meandering jet path.

[24] The deep, high-chlorophyll feature contained 2400 t of carbon, representing a substantial fraction of the productivity along a similarly sized length of the coast. It is argued that a few of these episodic events, i.e., injection of carbon from off the shelf to depth via mesoscale physical dynamics, per year would be sufficient to account for observed benthic mineralization rates within 300 km of the coast. Because of the ubiquity of filamentous features stretching seaward from coastal upwelling zones in the world's eastern boundary current regions, this mechanism for the flux of carbon off the shelf into the adjacent deep ocean must be considered when computing oceanic carbon budgets.

[25] **Acknowledgments.** We thank the Oregon State University Marine Technicians and the officers and crew of the R/V *Wecoma* for their skillful efforts at sea. T. Strub generously provided the satellite SST imagery. Support from the Office of Naval Research grants N00014-92J-1348, N00014-92J-1535, N00014-93-1-0730, N00014-95-1-0382, and N00014-97-1-0165 and from National Science Foundation grant OCE-9730639 is gratefully acknowledged.

References

- Barth, J. A., S. D. Pierce, and R. L. Smith, A separating coastal upwelling jet at Cape Blanco, Oregon and its connection to the California Current System, *Deep Sea Res., Part II*, 47, 783–810, 2000.
- Bernstein, R. L., L. Breaker, and R. Whitner, California Current eddy formation: Ship, air, and satellite results, *Science*, 195, 353–359, 1977.
- Bienfang, P., J. Szyper, and E. Laws, Sinking rate and pigment responses to light-limitation of a marine diatom: Implications to dynamics of chlorophyll maximum layers, *Oceanol. Acta*, 6, 55–62, 1982.
- Brink, K. H., and T. J. Cowles, The Coastal Transition Zone program, *J. Geophys. Res.*, 96, 14,637–14,647, 1991.
- Cowles, T. J., R. A. Desiderio, N. Potter, and C. Moore, Steep gradients in phytoplankton biomass in eastern boundary currents: Observations with a multi-excitation spectral fluorometer, *Eos Trans. AGU*, 75(3), *Ocean Sci. Meet. Suppl.*, 141, 1994.
- Haidvogel, D. B., A. Beckmann, and K. S. Hedstrom, Dynamic simulations of filament formation and evolution in the coastal transition zone, *J. Geophys. Res.*, 96, 15,017–15,040, 1991.
- Haynes, R., E. D. Barton, and I. Pilling, Development, persistence and variability of upwelling filaments off the Atlantic coast of Iberia, *J. Geophys. Res.*, 98, 22,681–22,692, 1993.
- Huyer, A., Hydrographic observations along the CODE Central Line off northern California, *J. Phys. Oceanogr.*, 14, 1647–1658, 1984.
- Huyer, A., J. A. Barth, P. M. Kosro, R. K. Shearman, and R. L. Smith, Upper-ocean water mass characteristics of the California Current, Summer 1993, *Deep Sea Res., Part II*, 45, 1411–1442, 1998.
- Jahnke, R. A., C. E. Reimers, and D. B. Craven, Intensification of organic matter at the sea floor near ocean margins, *Nature*, 348, 50–54, 1990.
- Kadko, D. C., L. Washburn, and B. Jones, Evidence of subduction within cold filaments of the northern California coastal transition zone, *J. Geophys. Res.*, 96, 14,909–14,926, 1991.
- Kelly, K. A., The influence of winds and topography on the sea surface temperature patterns over the northern California shelf, *J. Geophys. Res.*, 90, 11,783–11,798, 1985.
- Knauer, G. A., Productivity and new production of the oceanic systems, in *Interactions of C, N, P, and S Biogeochemical Cycles and Global Change*, edited by W. Wollast, F. T. MacKenzie, and L. Chou, pp. 211–231, Springer-Verlag, New York, 1993.
- Kosro, P. M., J. A. Barth, J. Fleischbein, A. Huyer, R. O'Malley, R. K. Shearman, and R. L. Smith, Seasoar and CTD observations during EBC cruises W9306A and W9308B, June to September 1993, *Data Rep. 160*, Coll. of Oceanic and Atmos. Sci., Oregon State Univ., Corvallis, 1995.
- Landry, M. R., and C. J. Lorenzen, Abundance, distribution, and grazing impact of zooplankton on the Washington shelf, in *Coastal Oceanography of Washington and Oregon*, edited by M. R. Landry and B. M. Hickey, pp. 175–210, Elsevier Sci., New York, 1989.
- Liu, K. K., K. Iseki, and S. Y. Chao, Continental margin carbon fluxes, in *The Changing Carbon Cycle*, edited by R. B. Hanson, H. W. Ducklow, and J. G. Field, pp. 187–239, Cambridge Univ. Press, New York, 2000.
- Longhurst, A. R., S. Sathyendranath, T. Platt, and C. M. Caverhill, An estimate of global primary production in the ocean from satellite radiometer data, *J. Plankton to Res.*, 17, 1245–1271, 1995.
- MacIassac, J. J., R. C. Dugdale, R. T. Barber, D. Blasco, and T. T. Packard, Primary production in an upwelling center, *Deep Sea Res., Part A*, 32, 503–529, 1985.
- Murphy, A. M., and T. J. Cowles, Effects of darkness on multi-excitation in vivo fluorescence and survival in a marine diatom, *Limnol. Oceanogr.*, 42, 1444–1453, 1997.
- Neori, A., O. Holm-Hansen, B. G. Mitchell, and D. A. Kiefer, Photoadaptation in marine phytoplankton, *Plant Physiol.*, 76, 518–524, 1984.
- Pollard, R. T., Frontal surveys with a towed profiling conductivity/temperature/depth measurement package (SeaSoar), *Nature*, 323, 433–435, 1986.
- Samelson, R., P. Barbour, J. A. Barth, S. Bielli, T. J. Boyd, D. Chelton, P. M. Kosro, M. Levine, E. Skillingstad, and J. Wilczak, Wind stress forcing of the Oregon coastal ocean during the 1999 upwelling season, *J. Geophys. Res.*, 107(C01), 10.1029/2001JC000900, 2002.
- Shearman, R. K., J. A. Barth, and P. M. Kosro, Diagnosis of the three-dimensional circulation associated with mesoscale motion in the California Current, *J. Phys. Oceanogr.*, 29, 651–670, 1999.
- Shillington, F. A., W. T. Peterson, L. Hutchings, T. A. Probyn, H. N. Waldron, and J. J. Agenba, A cool upwelling filament off Namibia, southwest Africa: Preliminary measurements of physical and biological properties, *Deep Sea Res., Part I*, 37, 1753–1772, 1990.
- Small, L. F., and D. W. Menzies, Patterns of primary productivity and biomass in a coastal upwelling region, *Deep Sea Res., Part A*, 28, 123–149, 1981.
- Smayda, T. J., The suspension and sinking of phytoplankton in the sea, *Oceanogr. Mar. Biol.*, 8, 353–414, 1970.
- Strub, P. T., J. M. Mesias, V. Montecino, J. Rutllant, and S. Salinas, Coastal ocean circulation off western South America, in *The Sea*, vol. 11, *The Global Coastal Ocean: Regional Studies and Syntheses*, edited by A. R. Robinson and K. H. Brink, pp. 273–313, John Wiley, New York, 1998.
- Swenson, M. S., P. P. Niiler, K. H. Brink, and M. R. Abbott, Drifter observations of a cold filament off Point Arena, California, in July 1988, *J. Geophys. Res.*, 97, 3593–3610, 1992.
- Traganza, E. D., J. C. Conrad, and L. C. Breaker, Satellite observations of a cyclonic upwelling system and giant plume in the California Current, in *Coastal Upwelling, Coastal Estuarine Sci.*, vol. 1, edited by F. A. Richards, pp. 228–241, AGU, Washington, DC, 1981.
- Walsh, J. J., G. T. Rowe, R. L. Iverson, and C. P. McRoy, Biological export of shelf carbon is a sink of the global CO₂ cycle, *Nature*, 291, 196–201, 1981.
- Washburn, L., D. C. Kadko, B. H. Jones, T. Hayward, P. M. Kosro, T. P. Stanton, S. Ramp, and T. Cowles, Water mass subduction and the transport of phytoplankton in a coastal upwelling system, *J. Geophys. Res.*, 96, 14,927–14,945, 1991.
- Wooster, W. S., and J. L. Reid, Eastern boundary currents, in *The Sea*, vol. 2, *The Composition of Sea Water: Comparative and Descriptive Oceanography*, edited by M. N. Hill, pp. 253–280, Wiley Interscience, New York, 1963.

J. A. Barth, T. J. Cowles, A. Huyer, P. M. Kosro, R. K. Shearman, and R. L. Smith, College of Oceanic and Atmospheric Sciences, Oregon State University, 104 Ocean Administration Building, Corvallis, OR 97331-5503, USA. (barth@coas.oregonstate.edu)

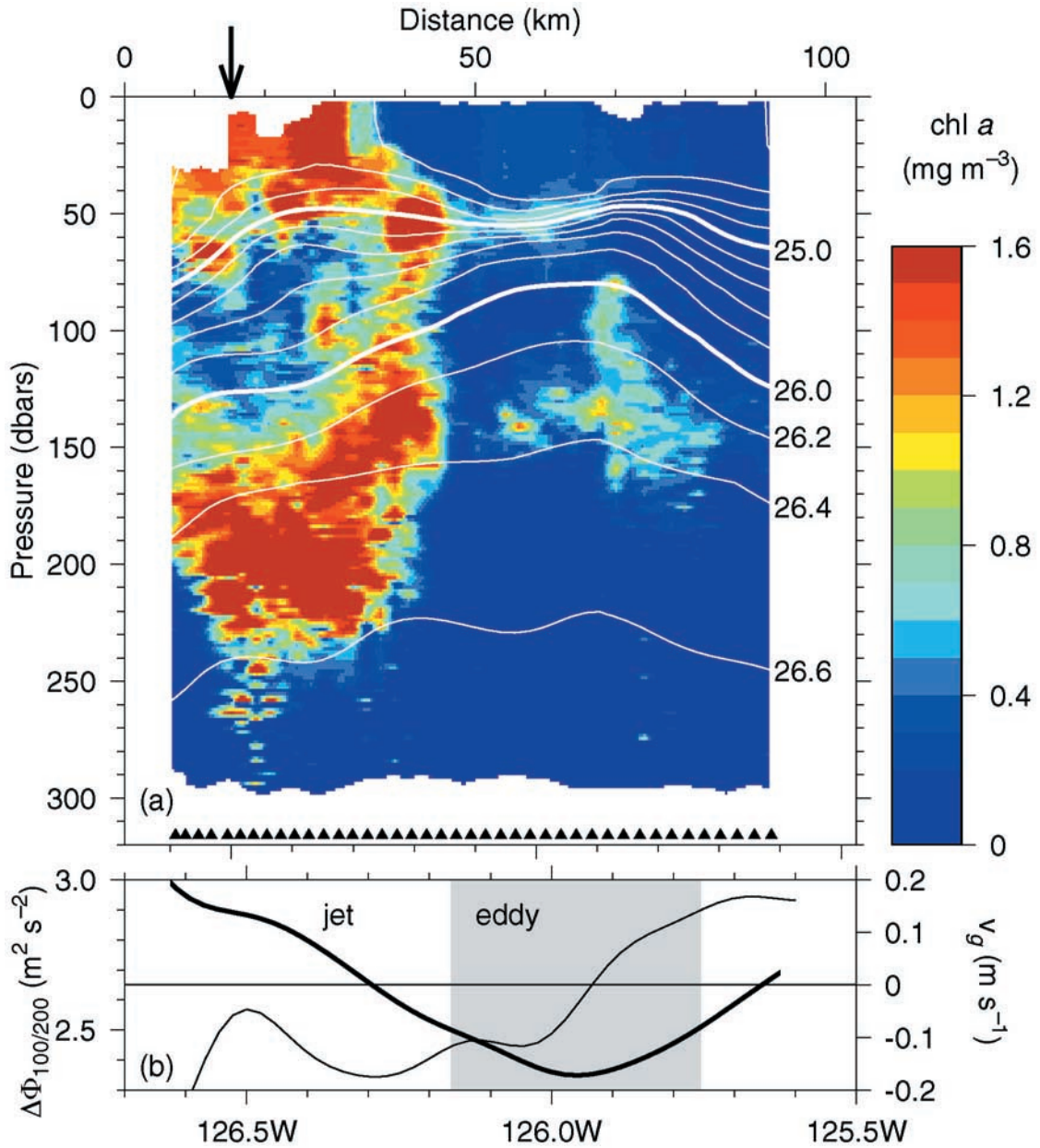


Figure 5. (a) Vertical section of Chl *a* (mg m^{-3}) derived from fluorescence (color) along 37.87°N on 30 June 1993 overlaid with contours of density anomaly (kg m^{-3}). The locations of each SeaSoar up-down cycle are indicated by triangles along the bottom. (b) Geopotential anomaly at 100 m, $\Delta\Phi_{100/200}$ ($\text{m}^2 \text{s}^{-2}$) (thick curve), and 100 m north-south geostrophic velocity, v_g (m s^{-1}), both referenced to acoustic Doppler current profiler velocity at 200 m, along 37.87°N.

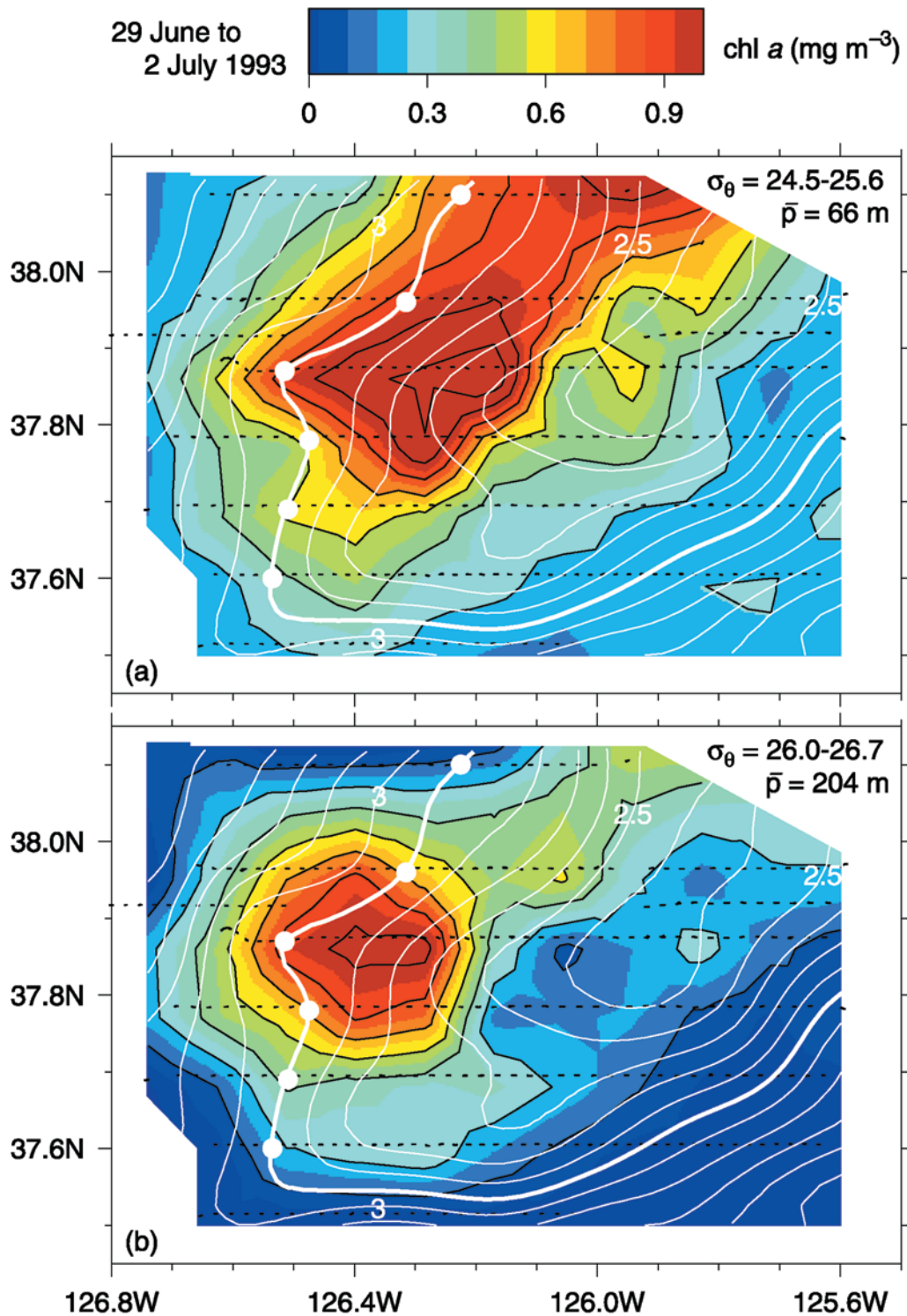


Figure 7. Chl *a* concentration (mg m^{-3}) derived from fluorescence (color and black contours) averaged between density anomaly surfaces (a) 24.5–25.6 and (b) 26.0–26.7 kg m^{-3} during 29 June to 2 July 1993 overlaid with contours of geopotential anomaly ($\text{m}^2 \text{s}^{-2}$) at 100 m referenced to acoustic Doppler current profiler velocity at 200 m (white contours). The thick geopotential anomaly contour ($2.9 \text{ m}^2 \text{s}^{-2}$) indicates the core of the meandering equatorward jet, and solid circles along this contour indicate locations of Chl *a* profiles shown in Figure 6.